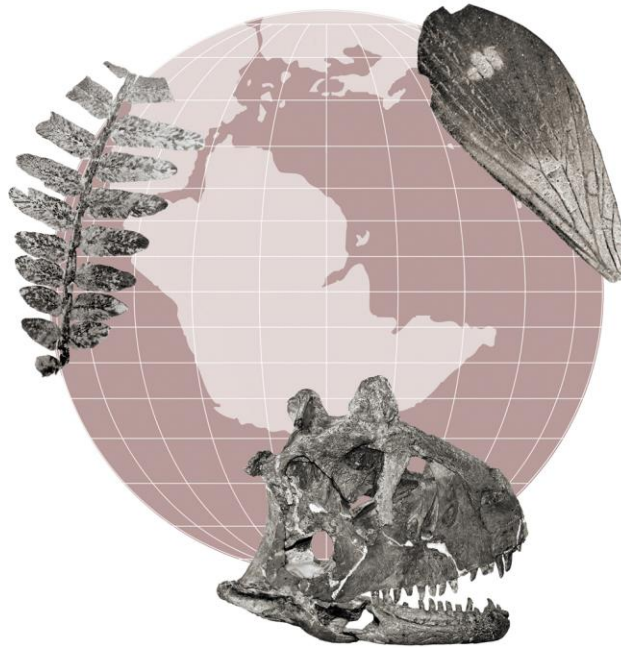




AMEGHINIANA

A GONDWANAN PALEONTOLOGICAL JOURNAL



This file is an uncorrected accepted manuscript (i.e., postprint). Please be aware that this version will change during the production process. This postprint will be removed once the paper is officially published. All legal disclaimers that apply to the journal pertain.

Submitted: 16 June 2024 - **Accepted:** 7 August 2025 - **Posted online:** 6 September 2025

To link and cite this article:

doi: [10.5710/AMGH.07.08.2025.3651](https://doi.org/10.5710/AMGH.07.08.2025.3651)

PLEASE SCROLL DOWN FOR ARTICLE

1 **PRELIMINARY REPORT OF ABELISAURID (DINOSAURIA, THEROPODA)**

2 **TOOTH AND TOOTH ATTACHMENT TISSUES**

3

4 IGNACIO A. CERDA^{1,2,3} AND JUAN D. PORFIRI^{4,5,6,7}

5 ¹Consejo Nacional de Investigación Ciencia y Técnica (CONICET), Argentina.

6 ²Instituto de Investigación en Paleobiología y Geología (IIPG), Universidad Nacional de

7 Río Negro (UNRN), Av. Gral. Julio Argentino Roca 1242, R8332 Gral. Roca, Río

8 Negro, Argentina.

9 ³Museo Carlos Ameghino, Belgrano 1700, Paraje Pichi Ruca (predio Marabunta),

10 R8300 Cipolletti, Río Negro, Argentina. nachocerda6@yahoo.com.ar

11 ⁴Museo de Ciencias Naturales, Secretaría de Extensión, Universidad Nacional del

12 Comahue, Buenos Aires 1400, Neuquén, Argentina.

13 ⁵Cátedra de Paleontología y Cátedra de Reptiles Mesozoicos, Facultad de Ingeniería,

14 Universidad Nacional del Comahue, Buenos Aires 1400, Neuquén, Argentina.

15 ⁶Museo del Desierto Patagónico de Añelo, Calle 1 y 6, Añelo, Neuquén, Argentina.

16 ⁷Instituto de Investigación en Tecnologías y Ciencias de la Ingeniería (IITCI) Consejo

17 Nacional de Investigaciones Científicas y Técnicas (CONICET) - Universidad Nacional

18 del Comahue (UNCo), Neuquén, Argentina. jporfiri@gmail.com

19

20

21 29 pag. (text + references); 5 figs.

22

23 Running Header: CERDA AND PORFIRI.: ABELISAURID TOOTH AND TOOTH

24 ATTACHMENT HISTOLOGY

25 Short Description: We present here a study focused on the histology of tooth and tooth
26 attachment tissue of an abelisaurid theropod.

27

28 Corresponding author: Ignacio Alejandro Cerda, nachocerda6@yahoo.com.ar

29 **Abstract.** Abelisauridae is a group of Late Cretaceous Gondwanan theropods
30 characterized by their bizarre skull anatomy, including a short, high and conspicuously
31 fused cranium ornamented with a rugose external surface. Studies of abelisaurid teeth
32 have focused on external crown morphology, leaving aspects of microstructure of tooth
33 and tooth attachments (i.e. periodontium) unexplored. These kinds of analyses are
34 essential to a more complete understanding of dental anatomy, development, and
35 evolution in theropod dinosaurs. In this contribution we study the microstructure of the
36 tooth and periodontium of an undetermined abelisaurid (MUCPv-1151) from the Upper
37 Cretaceous of Argentina. The histological analysis of a lower jaw fragment revealed the
38 presence of enamel, dentine with distinct growth lines and cementum in the teeth and
39 alveolar bone lining each alveolus. Although the dental microstructure is comparable to
40 that described for other theropod dinosaurs, there is significant variation in the thickness
41 of the growth lines in the dentine. Regarding periodontium histology, the data indicate
42 that abelisaurids had a gomphosis-type implantation, with a tissue distribution
43 comparable to that of other saurischians, including other non-avian theropods. However,
44 differences were identified in the thickness of the cellular cementum and the degree of
45 development of Sharpey's fibers in the cementum and alveolar bone. Histological data
46 reveal that the pattern of tooth formation and replacement in abelisaurids is comparable
47 with that of other amniotes. This contribution reveals that, irrespective of cranial
48 specializations reported for abelisaurid theropods, their tooth and periodontium,
49 alongside the pattern of tooth formation and replacement, are exhibits highly
50 conservative patterns.

51

52 **Keywords.** Dental growth rate. Dental histology. Periodontium. Tooth attachment.
53 Theropoda. Abelisauridae.

54 **Resumen.** ESTUDIO PRELIMINAR SOBRE DIENTES Y TEJIDOS DE INJERCIÓN
55 DENTAL DE ABELISÁURIDOS (DINOSAURIA, THEROPODA). Abelisauridae es
56 un grupo de terópodos gondwanicos del Cretácico Superior que se caracterizan por su
57 peculiar anatomía craneal, que incluye un cráneo corto, alto y visiblemente fusionado,
58 ornamentado con una superficie externa rugosa. Los estudios de los dientes de los
59 abelisáuridos se han centrado en la morfología externa de la corona, dejando sin
60 explorar aspectos de la microestructura dental y de sus tejidos de implante (ie., el
61 periodonto). Este tipo de análisis es esencial para una comprensión más completa de la
62 anatomía, el desarrollo y la evolución dental en los dinosaurios terópodos. En esta
63 contribución, estudiamos la microestructura dental y del periodonto de un abelisáurido
64 indeterminado (MUCPv-1151) del Cretácico Superior de Argentina. El análisis
65 histológico de un fragmento de mandíbula inferior reveló la presencia de esmalte,
66 dentina con líneas de crecimiento distintivas y cemento en los dientes, así como hueso
67 alveolar recubriendo cada alvéolo. Aunque la microestructura dental es comparable a la
68 descrita para otros dinosaurios terópodos, existe una variación significativa en el grosor
69 de las líneas de crecimiento en la dentina. Con respecto a la histología del periodonto,
70 los datos indican que los abelisáuridos tenían una implantación de tipo gonfosis, con
71 una distribución tisular comparable a la de otros saurísquios, incluyendo otros terópodos
72 no avianos. Sin embargo, se identificaron diferencias en el grosor del cemento celular y
73 el grado de desarrollo de las fibras de Sharpey en el cemento y el hueso alveolar. Los
74 datos histológicos revelan que el patrón de formación y reemplazo dental en los
75 abelisáuridos es comparable al de otros amniotas. Esta contribución revela que,
76 independientemente de las especializaciones craneales reportadas para los terópodos
77 abelisáuridos, sus dientes y su periodonto, junto con el patrón de formación y reemplazo
78 dental, exhiben patrones altamente conservativos.

79 **Palabras clave.** Tasa de crecimiento dental. Histología dental. Periodonto. Anclaje
80 dental. Theropoda. Abelisauridae.

81

82 ABELISAURIDAE IS A GROUP OF LATE CRETACEOUS GONDWANAN THEROPODS, NAMED BY
83 BONAPARTE AND NOVAS (1985) TO INCLUDE THE GENUS *ABELISAURUS* FROM THE
84 ARGENTINEAN PATAGONIA. This clade includes a large number of forms found in South
85 America, Africa, Madagascar, India, and also southern Europe (Bonaparte, 1991, 1996;
86 Novas *et al.*, 2013; Tortosa *et al.*, 2014). Abelisaurids are characterized by their highly
87 reduced forelimbs and a bizarre skull anatomy, including a short, high and
88 conspicuously fused cranium ornamented with a rugose external surface that evolved, in
89 some cases, horns or domes on the parietal roof (Bonaparte, 1991; Sampson, 1998;
90 Sampson & Witmer, 2007; Novas, 2009; Novas *et al.*, 2013; Zaher *et al.*, 2020; Cerroni
91 *et al.*, 2022). Similar to most of the non-avian theropods (Brink *et al.* 2015),
92 abelisaurids were carnivorous dinosaurs with polyphyodont dentitions with typical
93 ziphodont tooth morphology inserted in distinct alveoli. Although the dental anatomy of
94 abelisaurid theropods has been thoroughly analyzed in some taxa (*e.g.*, *Majungasaurus*
95 *crenatissimus*, Smith, 2007), information regarding tooth microstructure and tooth
96 attachment in this clade are still poorly explored.

97 To date, dental histology of abelisaurid theropods has been only partially studied
98 by D’Emic *et al.* (2019), who specifically studied the incremental lines of von Ebner in
99 *Majungasaurus crenatissimus*. Von Ebner lines are daily formed growth marks present
100 in the dentin (Erickson, 1996a, 1996b). Combining data from CT and histology, D’Emic
101 *et al.* (2019) analyzed the tooth formation and replacement rates in *Majungasaurus*
102 *crenatissimus* using both the tooth size and the von Ebner spacing. The replacement
103 rates in this taxon were interpreted as being higher than that of other non-avian
104 theropods. The estimation of tooth formation rates using spacing between von Ebner
105 lines has been also conducted in other sauropsids, including, for example, lepidosaurs,

106 sauropterygians and crocodyliforms (*e.g.*, Gren & Lidgren, 2013; Kear *et al.*, 2017;
107 Ricart *et al.*, 2019; Navarro *et al.*, 2022).

108 In the case of the tooth attachment tissues (*i.e.*, periodontium), these have not
109 been analyzed in Abelisauridae. Furthermore, our current knowledge about the structure
110 of the periodontium in other non-avian theropod dinosaurs is still very scarce. To date,
111 the only contributions in this regard have been conducted on the Triassic basal
112 neotheropod *Coelophysis bauri* and the tetanurans *Allosaurus fragilis* and *Gorgosaurus*
113 sp. (Reid, 1996; Fong *et al.*, 2016; LeBlanc *et al.*, 2016a, 2017b). As reported for other
114 dinosaurs (*e.g.*, García & Zurriaguz, 2016; LeBlanc *et al.*, 2016a, 2017b; Bramble *et al.*,
115 2017; Chen *et al.*, 2018), the periodontium of non-avian theropods is composed of three
116 specific tissues: root cementum, alveolar bone, and periodontal ligament (Reid, 1996;
117 Fong *et al.*, 2016; LeBlanc *et al.*, 2016a, 2017b). This tripartite condition represents the
118 plesiomorphic condition for Amniota (*e.g.*, LeBlanc & Reiz, 2013; LeBlanc *et al.*,
119 2016b, 2017a, 2017b, 2018). Despite the conservative nature of the periodontal tissue
120 histology, changes in the spatial distribution, degree of development and rates of
121 formation of these tissues has resulted in diverse tooth attachment geometries,
122 replacement modes, and bone architectures supporting the dentition in vertebrates (*e.g.*,
123 LeBlanc *et al.*, 2016a, 2020). In general terms, the histological study of the
124 periodontium has yielded valuable insights into the paleoecology, palaeobiology and
125 systematics of extinct groups (*e.g.*, Caldwell *et al.* 2003; Budney *et al.*, 2006; Maxwell
126 *et al.*, 2011a, 2011b; Snyder *et al.*, 2020, Dumont *et al.*, 2016; LeBlanc *et al.*, 2017a,
127 2020; 2021; 2023; Chen *et al.*, 2018; Mestriner *et al.*, 2021; Navarro *et al.*, 2022; Cerda
128 & Codorníu, 2023).

129 In this contribution we describe and interpret the microstructure of the tooth and
130 tooth attachment tissues of an undetermined abelisaurid (MUCPv-1151) from the Upper

131 Cretaceous of Argentina (Porfiri, *et al.*, 2006; 2009). Taking into account the current
132 knowledge about tooth and tooth attachment histology of vertebrates, the main aims of
133 this preliminary study are: 1- to determine if the high growth rate of tooth formation
134 reported for *Majungasaurus crenatissimus* is widespread in other abelisaurids; 2- to
135 characterize the periodontal histology of abelisaurids, using MUCPv-1151 as an
136 exemplar; 3- to examine and compare the tooth attachment of abelisaurids with other
137 archosaurs, evaluating the hypothesis of conservatism in the microstructural and spatial
138 distribution of the involved structures. This corresponds to the first histological study on
139 tooth attachment tissue for Ceratosauria.

140

141 **MATERIAL AND METHODS**

142 A fragment of a lower jaw from an incomplete skull (MUCPv-1151) was sampled for
143 histological analysis (Figure 1). The sample corresponds to a partial skeleton recovered
144 from the Upper Cretaceous (Cenomanian) outcrops of the Candeleros Formation, at
145 Aguada Pichana locality (170 Km northwest from Neuquén Province, Patagonia
146 Argentina). Taxonomical assignment of MUCPv-1151 to Abelisauridae has been
147 provided by Lamanna *et al.* (2019). A total of five thin sections, three transversal
148 (perpendicular to the tooth row) and two coronal (parallel to the tooth row in a
149 labiolingual plane), were obtained for histological analysis (Figure 1). Thin sections
150 were prepared at the petrographic laboratory of Universidad Nacional de San Luis (San
151 Luis, Argentina), using standard methods detailed by Cerda & Chinsamy (2012).
152 Nomenclature and definitions of histological structures used in this study follow
153 Francillon-Vieillot *et al.* (1990) and LeBlanc *et al.* (2017b). Nomenclature for tooth
154 implantation, attachment, and replacement follows LeBlanc *et al.*, (2017b) and Bertin *et*
155 *al.* (2018).

156

157 **RESULTS**

158 The sampled portion of the mandible is formed by the dentary, which has lost the most
159 of the functional tooth crowns. The lateral (labial) wall of the dentary is higher than the
160 medial (lingual) one due the absence of interdental plates in the sample. The teeth are
161 deeply implanted in distinct alveoli that reach the ventral portion of the dentary (Figure
162 2). Each alveolus contains one functional and at least one replacement tooth. Although
163 the roots and crowns of both functional and replacement teeth located inside the alveoli
164 have suffered from crushing, their original position can still be determined. In this
165 regard, the replacement teeth are located lingual to the functional teeth (Figure 3.1-3.4).
166 The apical portion of the functional tooth roots appear to be partially resorbed. The
167 labial margins of the alveoli at the deeper portion of the dentary (i.e. distal to the
168 occlusal margin) exhibit shallow resorption bays, here interpreted as replacement crypts
169 (Figure 3 .3).

170 Thin sections reveal a thin (32-48 μm) layer of enamel capping the tooth crowns (Figure
171 4.1-4.3). These measurements where mostly obtained from the crown of the
172 replacement tooth. Enamel exhibits a strong birefringence under cross-polarized light,
173 however the pattern is not homogeneous. In this regard, the enamel layer is formed by
174 distinct thin and columnar structures that exhibits different pattern of birefringence
175 (Figure 4.2, 4.3). The bulk of the teeth is formed by orthodentine (hereafter referred to
176 as dentine), which contains long tubules that would have housed the odontoblast
177 processes and occasional nerve filaments extending radially from the pulp cavity
178 towards the outer surface of the tooth. Dentine tubules extend into the dentine cores of
179 the serrations (denticles) (Figure 4.1). These tubules are less evident near the dentine-
180 enamel junction. The dentine appearance in this region is in some cases irregular and

181 possibly corresponds with globular dentine (Figure 4.2) (Brink *et al.*, 2015). Globular
182 dentine is, however, not evident in root dentine. The dentine exhibits a stratified pattern
183 of dark and light concentric bands (Figure 4.4-4.9). Due to diagenetic alteration, these
184 bands were only partially preserved in the sampled teeth. We measured the distance
185 between successive bands in different points of the sectioned teeth (77 measurements).
186 Due the banding nature of these histological structures, the thickness of successive
187 bands was considered as the distance between the inner margins of two consecutive
188 dark bands. We obtained an average thickness of 34 μm (SD $\pm 14 \mu\text{m}$) with a range of
189 variation between 9 and 63 μm . It must be noted that the distance between bands was
190 particularly short (*e.g.*, 10-13 μm) in some instances (*e.g.*, in the crown of the
191 replacement tooth showed in the Figure 4.9).

192 The dentine of the roots is lined by cellular cementum (Figure 5.1-5.3). The same
193 contain ovoid cementocyte lacunae. Cellular cementum is birefringent under polarized
194 light. Extinction pattern reveals that collagenous fibers were oriented perpendicular to
195 the root surface. The thickness of the cellular cementum is rather homogenous, ranging
196 between 52 and 60 μm . No evident Sharpey's fibers are recorded in the cellular
197 cementum.

198 A distinct band of birefringent, acellular tissue is present between the cellular cementum
199 and the dentine (Figure 5.2, 5.3). This tissue is actually composed by two thin layers
200 which exhibit tenuous differences with regard to the degree of birefringence. The layer
201 adjacent to the acellular cementum is the one with a more pronounced birefringence and
202 is interpreted as acellular cementum. The second, less birefringent layer appears to
203 correspond with the hyaline layer of the dentine (layer or of Hopewell-Smith)
204 (Nimoshini *et al.*, 2021).

205 Each alveolus is lined by a distinct layer of alveolar bone, which is separated from the
206 jawbone by a reversal line (Figure 5.4-5.6). The alveolar bone is formed by a well
207 vascularized woven bone matrix, with abundant and densely grouped osteocyte lacunae
208 arranged in no recognizable pattern. Vascular canals do not exhibit a particular
209 arrangement. The alveolar bone contains simple vascular canals and occasional primary
210 osteons, as indicated by the presence of lamellar bone lining the canals. Distinct
211 Sharpey's fibers are absent in the alveolar bone.

212 The jaw bone, dentary in this case, is composed of highly remodeled compact bone
213 (Figure 5.7-5.10). Secondary osteons, formed during several events of resorption and
214 new bone deposition, are mainly aligned parallel to the dentary main axis (i.e.,
215 anteroposterior/mesiodistal alignment). A slight variation to this pattern is observed in
216 the outer cortex of the lingual side of the dentary, toward the occlusal margin. Here
217 some groups of secondary osteons exhibits an alignment perpendicular to the dentary
218 main axis (Figure 5.9). The labial margins show a distinct appearance which is
219 characterized by the presence of ridges and valleys, reflecting some degree of
220 ornamentation in this side of the element (Figure 5.10, 5.11). Primary bone is preserved
221 in the outermost portion of the labial cortex (Figure 5.11).The same is formed by poorly
222 vascularized parallel fibered bone and contains several lines of arrested growth.

223 Sharpey's fibers are particularly abundant in this part of the cortex (Figure 5.11).

224 Transversal sections reveal that each tooth is separated by an hourglass-shaped wall of
225 interdental bone in cross-section (Figure 5.12). As occur in the lingual and labial walls
226 of the dentary, the interdental bone is entirely remodeled. The secondary osteons
227 constituting the interdental bone appears to be mostly arranged oblique to both
228 mesiodistal and labiolingual axis of the dentary (Figure 5.12).

229

230 **DISCUSSION**

231 **Dentinal growth marks**

232 An evident stratified pattern of dark and light concentric bands was recorded in the
233 dentine of the sectioned teeth of MUCPv-1151. At first instance, the bands appear to
234 correspond to the increment lines of von Ebner. However the variation in their thickness
235 (i.e. distance between the inner margins of two consecutive dark bands) raises doubts
236 about their nature. The thickness of the increment lines has been reported for numerous
237 vertebrate groups (*e.g.*, Erickson, 1996a, 1996b, Gren & Lidgren, 2013; García &
238 Zurriaguz, 2016; D’Emic *et al.*, 2013, 2024; Kear *et al.*, 2017; Chen *et al.*, 2018, 2023;
239 Whitney & Sidor, 2020; Navarro *et al.*, 2022; Maho & Reiz, 2024), including non-avian
240 theropods (Erickson, 1996b; Button *et al.* 2017; D’Emic *et al.*, 2019; Heckeberg &
241 Rauhut, 2020) and toothed birds (Dumont *et al.*, 2016). In abelisaurids, the thickness of
242 the increment lines reported by D’Emic *et al.* (2019) for *Majungasaurus crenatissimus*
243 is $18 \pm 5 \mu\text{m}$, which fall within the range of other archosaurs. This value does not differ
244 significantly from the obtained for *Ceratosaurus* ($14 \pm 3 \mu\text{m}$), the only non-abelisaurid
245 ceratosaur for which incremental lines of von Ebner lines have measured. Button *et al.*
246 (2017) indicated that the average of dentine deposition in Dinosauria resides within a
247 narrow range between 10-20 μm per day. Since incremental lines of von Ebner are
248 formed daily, this range can be considered as a direct indicator of dentine incremental
249 rates for dinosaurs. These values depart from the obtained from MUCPv-1151, which
250 has a higher thickness average (34 μm), with an important standard deviation ($\pm 14 \mu\text{m}$).
251 Furthermore, while the minimum thickness value in MUCPv-1151 (9 μm) resembles the
252 expected values, the maximum (63 μm) far exceeds it. This discrepancy may be due to
253 different, non-mutually exclusive factors. First, while the most closely grouped marks
254 could indeed correspond to von Ebner lines, the thicker increments possibly represent

255 Andresen lines. Andresen lines have been described in several vertebrates (*e.g.*, Scheyer
256 & Moser, 2011; Gren & Lidgren, 2013; Kear *et al.*, 2017) and correspond to long-
257 period growth marks regularly deposited after several days (*e.g.*, 6-10 in humans)
258 (Berkovitz & Shellis, 2016). Since most thickness measurements tend to cluster within
259 two distinct intervals (10-19 μm and 34-43 μm), these could correspond to the average
260 thickness between von Ebner lines and Andresen lines, respectively. However, it should
261 be noted that in those cases where Andresen lines are reported, these are superimposed
262 on the von Ebner lines (*e.g.*, Scheyer & Moser, 2011; Gren & Lidgren, 2013; Kear *et*
263 *al.*, 2017), something that is not evident in MUCPv-1151. The section plane is another
264 factor that could influence the strong variation regarding growth line thickness in the
265 specimen here analyzed. Kosch & Zanno (2020) showed that the section plane not only
266 affects the count of dentin increment lines, but can also affect their spacing. Given the
267 enormous variation in the growth marks thickness and the lack of certainty regarding
268 their nature (*i.e.*, whether they are all von Ebner lines or if Andresen lines are also
269 included), we refrain from make inferences regarding the rate of tooth formation in
270 MUCPv-1151.

271 **Tooth attachment tissues**

272 The existence of a periodontal space between the cellular cementum and the alveolar
273 bone in MUCPv-1151 indicates that, similar to most archosaurs (*e.g.*, García &
274 Zurriaguz, 2016; Fong *et al.*, 2016; LeBlanc *et al.*, 2017b; Chen *et al.*, 2018), tooth
275 attachment in abelisaurids corresponds to gomphosis. Gomphosis is characterized by the
276 presence of three attachment tissues: cementum (cellular and acellular), alveolar bone
277 and periodontal ligament (Bertin, 2016; LeBlanc *et al.*, 2017b). Although this type of
278 implantation is highly conserved in terms of the tissue types involved, the amount and
279 arrangement of these tissues can generate highly specialized patterns within lineages

280 (e.g., LeBlanc *et al.*, 2017b; Bramble *et al.*, 2017; Navarro *et al.*, 2022). In the case of
281 non-avian theropods, the few studies conducted on the subject show a basic condition in
282 which the roots are symmetrically covered by cellular and acellular cementum and the
283 alveolus is lined by alveolar bone (e.g., Reid, 1996; Fong *et al.*, 2016; LeBlanc *et al.*,
284 2017). This condition is reported here in MUCPv-1151, revealing that, irrespective of
285 cranial specializations reported for abelisaurid theropods, their tooth implantation
286 exhibits a conserved pattern with respect to Theropoda more broadly.. Despite the
287 general resemblance regarding tooth implantation tissues among non-avian theropods,
288 some differences are recorded in specific features. In this regard, the cellular cementum
289 thickness in MUCPv-1151 (52-60 μm) is comparable with the reported for *Coelophysis*
290 (50-55 μm) but noticeably thinner than the described for *Gorgosaurus* (150-175 μm)
291 (Fong *et al.*, 2016; LeBlanc *et al.*, 2017b). Since serial sections through the tooth roots
292 of these theropods revealed no detectable differences in cementum thickness along the
293 roots (Fong *et al.*, 2016; LeBlanc *et al.*, 2017b), the recorded variation among different
294 taxa does not appear to be related with the position of the root examined. Instead, the
295 cellular cementum thickness could be just tooth size-dependent, given the large size of
296 *Gorgosaurus* in comparison with *Coelophysis* and MUCPv-1151. This possible causal
297 relationship is supported by the reports of toothed birds as *Hesperornis regalis*, where
298 the cellular cementum thickness is less than 20 μm (figure 7.c in Dumont *et al.*, 2016).
299 It must be noted, however, that the cellular cementum thickness is possibly related with
300 other factors than tooth size in other archosaurs lineages. For example, Navarro *et al.*
301 (2022) considered that the relatively thicker cellular cementum found among
302 Mesoeucrocodylia, at least in comparison with other archosaurs, is possible related with
303 the increased bite forces.

304 Regarding alveolar bone, the distribution and fine structure of this tissue in MUCPv-
305 1151 are comparable not only with that reported for other non-avian theropods, such as
306 *Allosaurus*, *Coelophysis* and *Gorgosaurus* (Reid, 1996; Fong *et al.*, 2016; LeBlanc *et*
307 *al.*, 2017b), but also sauropod dinosaurs (García & Zurriaguz, 2016). The presence of
308 highly vascularized woven fibered bone forming the alveolar bone is not a feature
309 restricted to saurischian dinosaurs, since the same has been reported even for non
310 amniote tetrapods (LeBlanc & Reiz, 2013).

311 As previously mentioned, in gomphosis, a non-mineralized periodontal ligament
312 anchors into root cementum coating each tooth and into the alveolar bone forming each
313 tooth socket (Bertin *et al.*, 2018; LeBlanc, *et al.*, 2017b). The portion of the periodontal
314 ligament inserted into the cementum and the alveolar bone is mineralized, commonly
315 leaving distinct extrinsic Sharpey's fibers in the matrix (*e.g.*, LeBlanc, *et al.*, 2017b).

316 These extrinsic fibers, however, are not as evident in MUCPv-1151 as in other
317 archosaurs as notosuchian crocodyliforms (Navarro *et al.*, 2022) or early dinosauriforms
318 (Mestrimmer *et al.*, 2021). Whereas Sharpey's fibers are not recorded in the alveolar bone
319 of MUCPv-1151, they appear to be faintly grouped in the cellular cementum, as
320 evidenced by the extinction pattern observed in this tissue under polarized light. This
321 pattern is similar to the observed in the cellular cementum and alveolar bone of
322 *Coelophysis* (figure 3d in Fong *et al.*, 2016; figure 1a, b in LeBlanc *et al.*, 2017b) but
323 differs from the reported for *Gorgosaurus*, where the Sharpey's fibers are much more
324 evident in these tissues (figure 1c and d in LeBlanc *et al.*, 2017b). Although these
325 variations could be due to preservation artifacts, this seems rather improbable since
326 Sharpey's fibers, possibly related with the periosteum of dermal tissue, are well
327 preserved in the jaw bone (Figure 411). The poor development of Sharpey's fibers in
328 MUCPv-1151 (and possibly *Coelophysis*) is then possibly related to the intrinsic nature

329 of the periodontal ligament and the mineralization processes of the same. On this
330 regard, it must be noted that in some cases Sharpey' fibers are not clearly evident in the
331 cementum even when the non-mineralized portion of the periodontal ligament are
332 distinct in the section (*e.g.*, LeBlanc *et al.*, 2017a).

333

334 **Tooth replacement sequence**

335 The thin sections obtained from MUCPv-1151 allow us to infer the sequence of tooth
336 development and mode of replacement in an abelisaurid theropod. The position of the
337 functional and replacement teeth within the same alveolus reveals that, as reported for
338 most other amniotes, including non-avian dinosaurs (*e.g.*, Edmund, 1960; Fong *et al.*,
339 2016; Chen *et al.*, 2018), newly formed teeth develop lingual to the functional teeth
340 (Figure 3). Distinct resorption spaces located in the lingual side of the dentary are here
341 interpreted as replacement crypts and correspond to the spaces where the new
342 replacement teeth began to form. Replacement crypts in the lingual side of the tooth
343 bearing bone have been described in other non-avian saurischians (Reid, 1996; Fong *et*
344 *al.*, 2016; Leblanc *et al.*, 2017b). Following the pattern inferred by Fong *et al.* (2016)
345 and LeBlanc *et al.* (2017b) for non-avian theropods, it appears that the developing tooth
346 in MUCPv-1151 first forms within the replacement crypt. As the replacement tooth
347 matured, it migrated labially, resorbing the lingual surface of the functional tooth root.
348 In a more advanced stage of development, the replacement tooth occupies fully the pulp
349 cavity of the functioning tooth, which is followed by shedding of the older tooth. An
350 exception to this pattern has been reported for crocodylians, where, except for hatching
351 individuals, the replacement crypts are positioned underneath the roots of the functional
352 teeth, albeit very slightly lingual to the midline of the functional tooth root (LeBlanc *et*

353 *al.*, 2017b). The pattern of tooth replacement sequence in abelisaurids appears to be
354 conservative regarding not only non-avian theropods, but also amniotes in general.

355 **CONCLUSIONS AND FUTURE PERSPECTIVES**

356 In this study, we present results on tooth and tooth attachment histology of an
357 abelisaurid theropod. Although the dental microstructure is comparable to that described
358 for other theropod dinosaurs, there is significant variation in the thickness of the growth
359 lines in the dentine. It is not clear whether these lines correspond to incremental lines of
360 von Ebner or Andresen lines. We consider that new thin sections analyses on
361 abelisaurid theropod teeth are necessary for the accurate interpretation of these lines and
362 the cause of their thickness variation. These new analyses should be performed from
363 sections oriented in a mesiodistal plane, since these have proven to be the most reliable
364 for the study of these lines in theropod dinosaurs (*e.g.* D'Emic *et al.*, 2019).
365 Furthermore, thin sections obtained from mesiodistal plane will allow the adjustment of
366 the proposed models for tooth replacement rates proposed for non-avian theropods
367 (D'Emic *et al.*, 2019). Regarding tooth attachment histology, the data indicate that
368 abelisaurids, like other dinosaurs, had a gomphosis-type implantation, with a tissue
369 distribution comparable to that of other saurischians. However, differences were
370 identified in the thickness of the cellular cementum layer and the degree of development
371 of Sharpey's fibers in the cementum and alveolar bone. The hypotheses proposed here to
372 explain these variations should be tested in new studies that not only include more
373 individuals assigned to Abelisauridae, but also to other saurischian dinosaurs. Inclusion
374 of specimens of different ontogenetic stages is also desirable. Finally, although
375 histological data reveal that the pattern of tooth formation and replacement in
376 abelisaurids is comparable with that of other amniotes, new data based on CT analyses
377 will allow for a more in-depth and precise analysis of this.

378

379 **ACKNOWLEDGMENTS**

380 We would like to thank Mauricio Cerroni and Diego Pol for their invitation to
381 participate in the special volume of *Ameghiniana* “40th anniversary of Abelisauridae”.
382 The constructive comments of Aaron LeBlanc and Jordi Alexis Garcia Marsà have
383 greatly improved this manuscript. Funding for the collection and preparation of this
384 material was provided by the Museum of Natural Sciences (MUC) of the National
385 University of Comahue. We would like to thank all those who collaborated with the
386 paleontological work at Aguada Pichana, Neuquén. We would also like to thank the
387 field owners, Dora and Raúl Urrutia, for their continued support.

388

389 **REFERENCES**

- 390 Berkovitz, B. K., & Shellis, R. P. (2017). *The teeth of non-mammalian vertebrates*.
391 London, United Kingdom. Academic Press.
- 392 Bertin, T. J. C., Thivichon-Prince, B., LeBlanc, A. R. H., Caldwell, M. W., & Viriot, L.
393 (2018) Current perspectives on tooth implantation, attachment, and replacement in
394 Amniota. *Frontier in Physiology*, 9:1630. doi: 10.3389/fphys.2018.01630
- 395 Bonaparte, J. F. (1991). The gondwanian theropod families Abelisauridae and
396 Noasauridae. *Historical Biology*, 5(1), 1–25.
- 397 Bonaparte, J. F. (1996). Cretaceous tetrapods of Argentina. In G. Arratia (Ed.).
398 *Contributions of Southern South America to Vertebrate Paleontology* (pp. 73–
399 130). Münchner Geowissenschaftliche Abhandlungen (A)30. Verlag Dr. Friedrich
400 Pfeil, München.
- 401 Bonaparte, J. F., & Novas, F. E. (1985). *Abelisaurus comahuensis*, n.g., n.sp.,
402 Carnosauria del Cretácico Tardío de Patagonia. *Ameghiniana*, 21(2-4), 259–265.

403 Bramble, K., LeBlanc, A. R. H., Lamoureux, D. O., Wosik, M., & Currie, P. (2017)
404 Histological evidence for a dynamic dental battery in hadrosaurid dinosaurs.
405 *Scientific Reports*, 7, 15787. <https://doi.org/10.1038/s41598-017-16056-3>

406 Brink, K. S., Reisz, R. R., LeBlanc, A. R. H., Chang, R. S., Lee, Y. C., Chiang, C. C.,
407 Huang, T., & Evans, D. C. (2015). Developmental and evolutionary novelty in the
408 serrated teeth of theropod dinosaurs. *Scientific Reports*, 5, 12338.
409 <https://doi.org/10.1038/srep12338>

410 Budney, L. A., Caldwell, M. W., & Albino, A. (2006) Tooth socket histology in the
411 Cretaceous snake *Dinilysia*, with a review of amniote dental attachment tissues.
412 *Journal of Vertebrate Paleontology*, 26(1), 138–145.

413 Button, K., You, H., Kirkland, J. I., & Zanno, L. (2017). Incremental growth of
414 therizinosaurian dental tissues: Implications for dietary transitions in Theropoda.
415 *PeerJ*, 5, e4129. DOI 10.7717/peerj.4129

416 Caldwell, M. W., Budney, L. A., & Lamoureux, D. O. (2003) Histology of tooth
417 attachment tissues in the Late Cretaceous mosasaurid *Platecarpus*. *Journal of*
418 *Vertebrate Paleontology*, 23(3), 622–630.

419 Cerda, I. A., & Chinsamy, A. (2012) Biological implications of the bone microstructure
420 of the Late Cretaceous ornithopod dinosaur *Gasparinisaura cincosaltensis*.
421 *Journal of Vertebrate Paleontology*, 32(2), 355–368.

422 Cerda, I. A., & Codorníu, L. (2023) Palaeohistology reveals an unusual periodontium
423 and tooth implantation in a filter-feeding pterodactyloid pterosaur, *Pterodaustro*
424 *guinazui*, from the Lower Cretaceous of Argentina. *Journal of Anatomy*, 243(4),
425 579–589.

426 Cerroni, M. A., Canale, J. I., Novas, F. E., & Paulina-Carabajal, A. (2022). An
427 exceptional neurovascular system in abelisaurid theropod skull: new evidence
428 from *Skorpiovenator bustingorryi*. *Journal of Anatomy*, 240(4), 612–626.

429 Chen, J., LeBlanc, A. R. H., Jin, L., Huang, T., & Reisz, R. R. (2018). Tooth
430 development, histology, and enamel microstructure in *Changchunsaurus parvus*:
431 Implications for dental evolution in ornithomimid dinosaurs. *PLoS One*, 13(11),
432 e0205206. <https://doi.org/10.1371/journal.pone.0205206>

433 Chen, H., Li, Z., Jiang, S., Wu, Q., Gong, Y., Zhu, X., & Wang, X. (2023). A
434 preliminary analysis of dental microstructure in *Hamipterus* (Pterosauria,
435 Pterodactyloidea). *The Anatomical Record*, <https://doi.org/10.1002/ar.25289>

436 D'Emic, M. D., Finch, S. P., Britt, B. B., & Wilson Mantilla, J. A. (2024). Increased
437 sampling reveals the complex evolution of sauropod dinosaur tooth replacement
438 rates. *Journal of Anatomy*, <https://doi.org/10.1111/joa.14169>

439 D'Emic, M. D., O'Connor, P. M., Pascucci, T. R., Gavras, J. N., Mardakhayava, E., &
440 Lund, E. K. (2019). Evolution of high tooth replacement rates in theropod
441 dinosaurs. *PLoS One*, 14(11), e0224734. [https://doi.org/10.1371/journal.pone.](https://doi.org/10.1371/journal.pone.0224734)
442 [0224734](https://doi.org/10.1371/journal.pone.0224734)

443 D'Emic, M. D., Whitlock, J. A., Smith, K. M., Fisher, D. C., & Wilson, J. A. (2013).
444 Evolution of high tooth replacement rates in sauropod dinosaurs. *PLoS One*, 8(7),
445 e69235. <https://doi.org/10.1371/journal.pone.0069235>

446 Dumont, M., Tafforeau, P., Bertin, T., Bhullar, B. A., Field, D., Schulp, A., Strilisky,
447 B., Thivichon-Prince, B., Viriot, L., & Louchart, A. (2016). Synchrotron imaging
448 of dentition provides insights into the biology of *Hesperornis* and *Ichthyornis*, the
449 “last” toothed birds. *BMC Evolutionary Biology*, 16, 178. doi: 10.1186/s12862-
450 016-0753-6

451 Edmund, A. G. (1960) Tooth replacement phenomena in the lower vertebrates. *Life*
452 *Sciences Division Royal Ontario Museum Toronto Contributions*, 52, 1–190.

453 Erickson, G. M. (1996a) Incremental lines of von Ebner in dinosaurs and the assessment
454 of tooth replacement rates using growth line counts. *Proceedings of the National*
455 *Academy of Sciences of the United States of America*, 93(25), 14623–14627.

456 Erickson, G. M. (1996b) Daily deposition of dentine in juvenile *Alligator* and
457 assessment of tooth replacement rates using incremental line counts. *Journal of*
458 *Morphology*, 228(2), 189–194.

459 Fong, R. K. M., LeBlanc, A. R. H., Berman, D. S., & Reisz, R. R. (2016) Dental
460 histology of *Coelophysis bauri* and the evolution of tooth attachment tissues in
461 early dinosaurs: dinosaur dental histology. *Journal of Morphology*, 277(7), 916–
462 924.

463 Francillon-Vieillot, H., de Buffrénil, V., Castanet, J., Géraudie, J., Meunier, F. J., Sire,
464 J. Y., Zylberberg, L., & de Ricqlés, A. (1990) Microstructure and mineralization
465 of vertebrate skeletal tissues. In J. G. Carter (Ed.) *Skeletal biomineralization:*
466 *patterns, processes and evolutionary trends, Vol. 1.* (pp. 471–530). Van Nostrand
467 Reinhold, Nueva York.

468 García, R. A., & Zurriaguz, V. (2016). Histology of teeth and tooth attachment in
469 titanosaurs (Dinosauria; Sauropoda). *Cretaceous Research*, 57, 248–256.

470 Gren, J. A., & Lindgren, J. (2013). Dental histology of mosasaurs and a marine
471 crocodylian from the Campanian (Upper Cretaceous) of southern Sweden:
472 incremental growth lines and dentine formation rates. *Geological Magazine*,
473 151(1), 134–143.

474 Heckeberg, N. S., & Rauhut, O. W. (2020). Histology of spinosaurid dinosaur teeth
475 from the Albian-Cenomanian of Morocco: Implications for tooth replacement and

476 ecology. *Palaeontologia Electronica*, 23(3), a48.
477 <https://doi.org/10.26879/1041palaeo-electronica.org/content/2020/3170-histology->
478 of-spinosaurid-teeth

479 Kear, B. P., Larsson, D., Lindgren, J., & Kundrát, M. (2017) Exceptionally prolonged
480 tooth formation in elasmosaurid plesiosaurosaurs. *PLoS One*, 12(2), e0172759.
481 doi:10.1371/journal.pone.0172759

482 Kosch, J. C. D., & Zanno, L. E. (2020). Sampling impacts the assessment of tooth
483 growth and replacement rates in archosaurs: Implications for paleontological
484 studies. *PeerJ*, 8, e9918. <https://doi.org/10.7717/peerj.9918>

485 Lamanna, M., Porfiri, J. D., Dos Santos, D., Juárez Valieri, R. D., Gandossi, P. &
486 Baiano, M. (2019). A new and well-preserved early-diverging abelisaurid
487 (theropoda: Ceratosauria: Abelisauroida) from the early Cretaceous of Northern
488 Patagonia. *79 th Annual Meeting Society of Vertebrate Paleontology (SVP)*.
489 Brisbane, Queensland, Australia.

490 LeBlanc, A. R. H., Apesteguía, S., Larsson, H. C. E., & Caldwell, M. W. (2020) Unique
491 tooth morphology and prismatic enamel in Late Cretaceous sphenodontians from
492 Argentina. *Current Biology*, 4(9), 1755–1761.

493 LeBlanc, A. R. H., Brink, K. S., Cullen, T. M., & Reisz, R. R. (2017b) Evolutionary
494 implications of tooth attachment versus tooth implantation: a case study using
495 dinosaur, crocodylian, and mammal teeth. *Journal of Vertebrate Paleontology*,
496 37(5), e1354006.

497 LeBlanc, A. R. H., Brink, K. S., Whitney, M., Abdala, F., & Reisz, R. R. (2018) Dental
498 ontogeny in extinct synapsids reveals a complex evolutionary history of the
499 mammalian tooth attachment system. *Proceedings of the Royal Society B:*
500 *Biological Sciences*, 285, 20181792. <http://dx.doi.org/10.1098/rspb.2018.1792>

501 LeBlanc, A. R. H., Lamoureux, D. O., & Caldwell, M. W. (2017a). Mosasaurs and
502 snakes have a periodontal ligament: timing and extent of calcification, not tissue
503 complexity, determines tooth attachment mode in reptiles. *Journal of Anatomy*,
504 *231*(6), 869–885.

505 LeBlanc, A. R. H., Palci, A., Anthwal, N., Tucker A.S., Araújo, R., Pereira, M. F. C. &
506 Caldwell, M. W. (2023). A conserved tooth resorption mechanism in modern and
507 fossil snakes. *Nature Communications*, *14*, 742. [https://doi.org/10.1038/s41467-](https://doi.org/10.1038/s41467-023-36422-2)
508 [023-36422-2](https://doi.org/10.1038/s41467-023-36422-2)

509 LeBlanc, A. R. H., Paparella, I., Lamoureux, D. O., Doschak, M. R., & Caldwell, M. W.
510 (2021), Tooth attachment and pleurodont implantation in lizards: Histology,
511 development, and evolution. *Journal of Anatomy*, *238*(5), 1156–1178.

512 LeBlanc, A. R. H., & Reisz, R. R. (2013) Periodontal ligament, cementum, and alveolar
513 bone in the oldest herbivorous tetrapods, and their evolutionary significance.
514 *PLoS One*, *8*(9), e74697. <https://doi.org/10.1371/journal.pone.0074697>

515 LeBlanc, A. R. H., & Reisz, R. R., Evans, D. C., & Bailleul, A. M. (2016a) Ontogeny
516 reveals function and evolution of the hadrosaurid dinosaur dental battery. *BMC*
517 *Evolutionary Biology*, *16*, 152. doi:10.1186/s12862-016-0721-1

518 LeBlanc, A. R. H., & Reisz, R. R., Brink, K. S., & Abdala, F. (2016b) Mineralized
519 periodontia in extinct relatives of mammals shed light on the evolutionary history
520 of mineral homeostasis in periodontal tissue maintenance. *Journal of Clinical*
521 *Periodontology*, *43*(4), 323–332.

522 Maho, T., & Reisz, R. R. (2024) Exceptionally rapid tooth development and ontogenetic
523 changes in the feeding apparatus of the Komodo dragon. *PLoS One*, *19*(2),
524 e0295002. <https://doi.org/10.1371/journal.pone.0295002>

525 Maxwell, E. E., Caldwell, M. W., & Lamoureux, D. O. (2011a) Tooth histology,
526 attachment, and replacement in the Ichthyopterygia reviewed in an evolutionary
527 context. *Paläontologische Zeitschrift*, 86(1), 1–14.

528 Maxwell, E. E., Caldwell, M. W., & Lamoureux, D. O. (2011b) Tooth histology in the
529 Cretaceous ichthyosaur *Platypterygius australis*, and its significance for the
530 conservation and divergence of mineralized tooth tissues in amniotes. *Journal of*
531 *Morphology*, 272(2), 129–135.

532 Mestriner, G., LeBlanc, A. R. H., Nesbitt, S. J., Marsola, J. C. A., Irmis, R. B., Stock
533 Da-Rosa, A. A., Ribeiro, A. M., Ferigolo, J., & Langer, M. (2021) Histological
534 analysis of ankylotheodonty in Silesauridae (Archosauria: Dinosauriformes) and
535 its implications for the evolution of dinosaur tooth attachment. *The Anatomical*
536 *Record*, 305(2), 393–423.

537 Navarro, T., Cerda, I. A., Barrios, F. & Pol, D. (2022) Dental histology and attachment
538 tissues in *Notosuchus terrestris* (Crocodyliformes, Notosuchia): palaeobiological
539 implications. *Lethaia*, 55(1), 1–10.

540 Nimoshini, G., Ramadoss R., Swarnalakshmi, R., Vasanthi, V., Kumar, A.R. & Bose,
541 D. (2021). Hyaline layer of Hopewell-Smith: A morphometric and histochemical
542 analysis. *CODS Journal of Dentistry*, 13(1): 3–5.

543 Novas, F. E. (2009). *The age of dinosaurs in South America*. USA. Indiana University
544 Press.

545 Novas, F. E., Agnolín, F. L., Ezcurra, M. D., Porfiri, J. D., & Canale, J. I. (2013).
546 Evolution of the carnivorous dinosaurs during the Cretaceous: the evidence from
547 the Patagonia. *Cretaceous Research*, 45,174–215.

- 548 Porfiri, J. D., Gandossi, P., & Calvo, J.O. (2006). New material of Abelisauroida
549 (Theropoda) from Cenomanian of Patagonia, Argentina. *V Simposio Brasileiro de*
550 *Paleontología de Vertebrados*. Santa María, Brasil.
- 551 Porfiri, J. D., Gandossi, P., Calvo, J.O. & Dos Santos, D. (2009). A new abelisauroid
552 skeleton from the Late Cretaceous of Neuquén, NW Patagonia, Argentina. XXIV
553 *Jornadas Argentinas de Paleontología de Vertebrados* (pp. 52). San Rafael,
554 Mendoza.
- 555 Reid, R. E. H. (1996) Bone histology of the Cleveland-Lloyd dinosaurs and of
556 dinosaurs in general, Part I: introduction to bone tissues. *Brigham Young*
557 *University, Geological Studies*, 41, 25–71.
- 558 Ricart, R. S. D., Santucci, R. M., Andrade, M. B., Oliveira, C. E. M., Nava, W. R. &
559 Degrazia, G. F. (2019) Dental histology of three notosuchians (Crocodylomorpha)
560 from the Bauru Group, Upper Cretaceous, South-eastern Brazil. *Historical*
561 *Biology*, 33(7), 1012–1023.
- 562 Sampson, S. D. (1998) Predatory dinosaur remains from Madagascar: implications for
563 the Cretaceous biogeography of Gondwana. *Science*, 280, 1048–1051.
- 564 Sampson, S. D. & Witmer, L. M. (2007) Craniofacial anatomy of *Majungasaurus*
565 *crenatissimus* (Theropoda: Abelisauridae) from the Late Cretaceous of
566 Madagascar. *Journal of Vertebrate Paleontology*, 27(2), 32–102.
- 567 Scheyer, T. M, & Moser, M. (2011) Survival of the thinnest: rediscovery of Bauer's
568 (1898) ichthyosaur tooth sections from Upper Jurassic lithographic limestone
569 quarries, south Germany. *Swiss Journal of Geosciences*, 104(1), 147–157.
- 570 Smith, J. B. (2007) Dental morphology and variation in *Majungasaurus crenatissimus*
571 (Theropoda: Abelisauridae) from the Late Cretaceous of Madagascar. *Journal of*
572 *Vertebrate Paleontology*, 27(2), 103–126.

573 Snyder, A. J., LeBlanc, A. R. H., Jun, C., Bevitt, J. J., & Reisz, R. R. (2020) Thecodont
574 tooth attachment and replacement in bolosaurid parareptiles. *PeerJ*, 8, e9168.
575 <http://doi.org/10.7717/peerj.9168>

576 Tortosa, T., Buffetaut, E., Vialle, N., Dutour, Y., Turini, E., & Cheylan, G. (2014). A
577 new abelisaurid dinosaur from the Late Cretaceous of southern France:
578 palaeobiogeographical implications. *Annales de Paléontologie*, 100(1), 63–86.

579 Whitney, M.R., Sidor, C.A. (2020). Evidence of torpor in the tusks of *Lystrosaurus*
580 from the Early Triassic of Antarctica. *Communications Biology*, 3, 471.
581 <https://doi.org/10.1038/s42003-020-01207-6>

582 Zaher, H., Pol, D., Navarro, B. A., Delcourt, R., & Carvalho A. B. (2020). An Early
583 Cretaceous theropod dinosaur from Brazil sheds light on the cranial evolution of
584 the Abelisauridae. *Comptes Rendus Palevol*, 19(6), 101–115.

585

586

587 **Figure captions**

588 **Figure 1.** Fragment of the lower mandible of *Abelisauridae* indet. MUCPv-1151
589 sampled for histological analysis in **1**, labial; **2**, lingual; and **3**, occlusal views. Dashed
590 lines indicate the location and orientation of the thin sections. Inset numbers correspond
591 with the images showed in Figure 2. Abbreviations: **nvf**, neurovascular foramen. Scale
592 bar equals 10 mm. **-PLANED FOR A SINGLE COLUMN-**

593
594 **Figure 2.** Complete histological sections of *Abelisauridae* indet. MUCPv-1151. **1-4**,
595 transversal sections (anterior/mesial is to the left, and lingual towards the top of the
596 images). **5-7**, coronal sections (labial is to the left, and occlusal toward the top of the
597 images). The location of each section is indicated in the Figure 1. Numbered boxes
598 indicate the position of the images showed in the Figures 4 and 5. Scale bars equal 5
599 mm. **-PLANED FOR A SINGLE COLUMN-**

600
601 **Figure 3.** Location of replacement and functional teeth in *Abelisauridae* indet. MUCPv-
602 1151. **1-4**, Diagrammatic illustration of the complete transversal sections showed in
603 Figure 3.1-3.4 (anterior/mesial is to the left, and lingual towards the top of the images).
604 Whereas the jaw bone is represented in light gray, replacement and functional teeth are
605 in black and dark gray respectively. Black asterisk signal the position of a replacement
606 crypt. Roman numbers denote each individual alveolus. Scale bars equal 5 mm.

607 **-PLANED FOR A SINGLE COLUMN-**

608
609 **Figure 4.** Tooth histology of *Abelisauridae* indet. MUCPv-1151. **1-3**, general view (1)
610 and details (2, 3) of the tooth in transversal sections. Note the particular pattern of
611 birefringence of the enamel. The box inset in 1 represents the position of the detailed

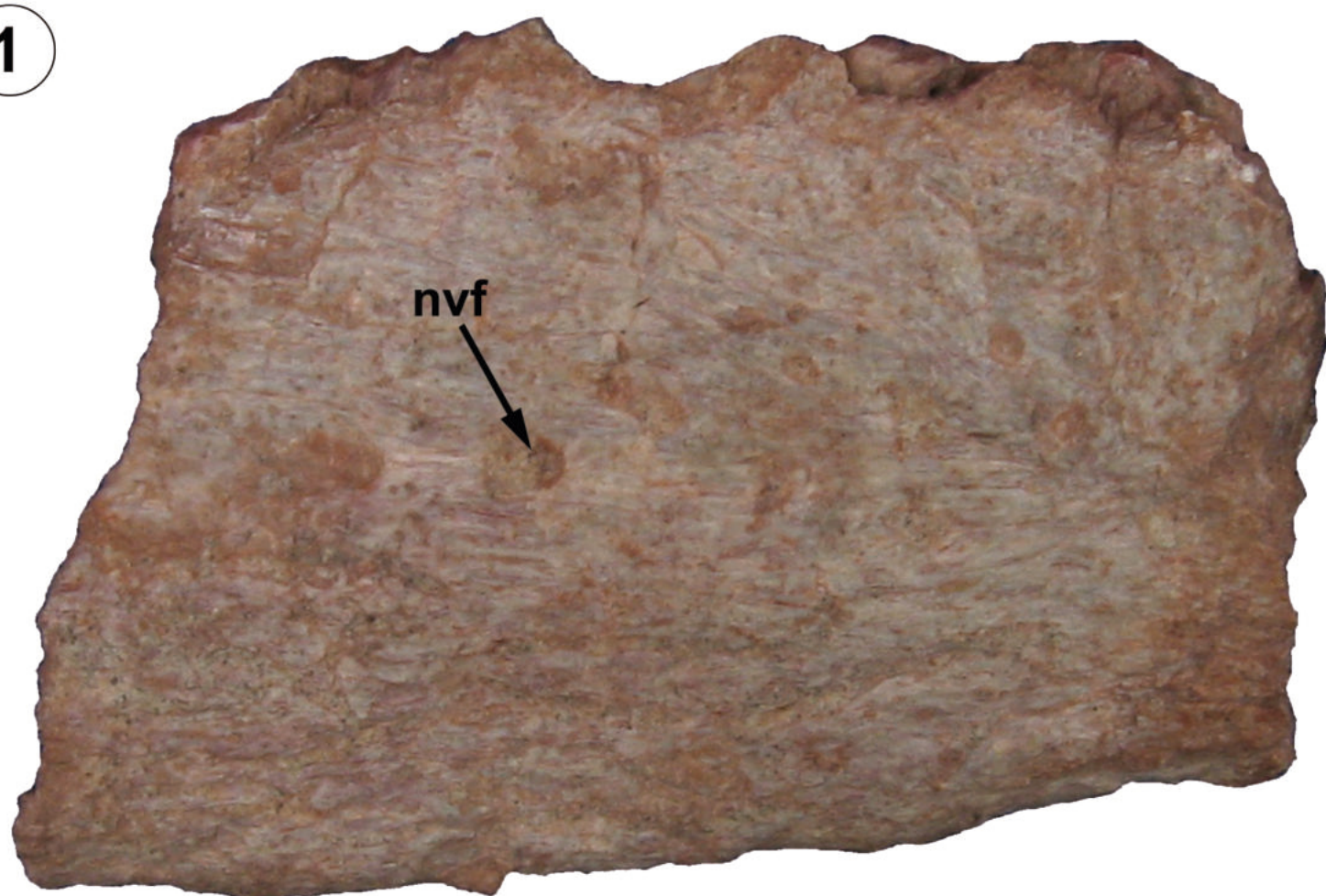
612 view showed in 2. **4-9**, detailed view of the dentine in both transversal (4-7) and coronal
613 (8, 9) sections. The images inset at the upper right corner correspond to the
614 enlargements of the areas indicated in each with the box. White arrowheads signal the
615 position of successive marks in the dentine. For ease of comparison, both the general
616 images and the details are shown on the same scale. 1, 4-9, 12: plane polarized light. 2,
617 3; cross polarized light with lambda compensator. Abbreviations: **de**, dentine; **dt**,
618 dentine tubules; **en**, enamel; **gd**, globular dentine; **td**, tooth denticle. Scale bars equal
619 0.2 mm (1, 4-9), 0.1 mm (2, 3). **-PLANNED FOR A DOUBLE COLUMN-**

620

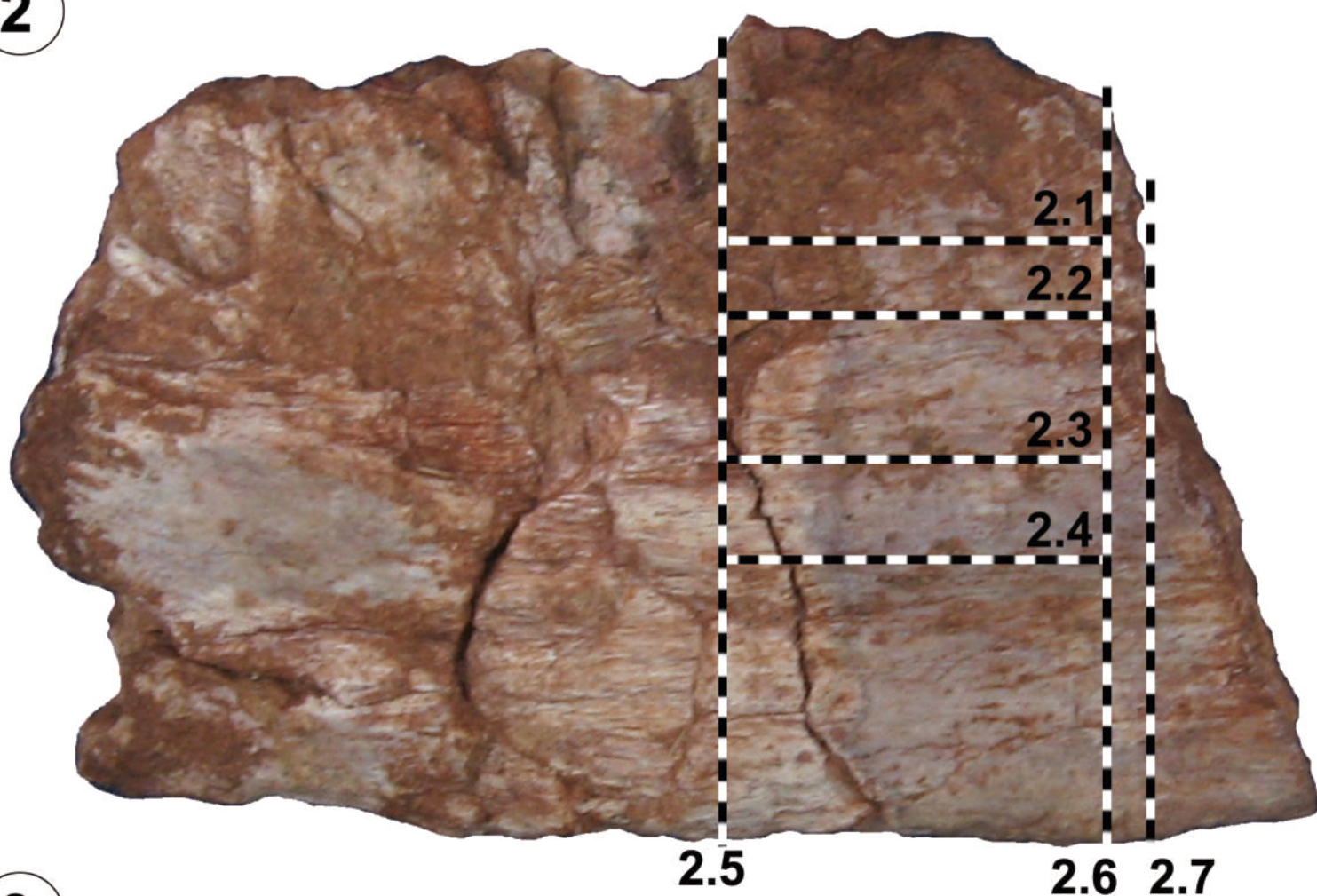
621 **Figure 5.** Histology of tooth and tooth attachment tissues of *Abelisauridae* indet.
622 MUCPv-1151. **1-3**, general view (1) and details (2, 3) of the tooth attachment tissues in
623 transversal section. The area showed in 2 and 3 correspond to the large box inset in 1. **4-**
624 **6**, alveolar bone preserved in different areas of the sample, including both transversal
625 (4, 6) and coronal (5) sections. The detailed view showed in 6 correspond to the small
626 inset box in 1. **7-9**, Haversian bone tissue in transversal (7) and coronal (8, 9) sections
627 of the dentary. Note the predominance of longitudinally oriented secondary osteons.
628 White arrowhead in 9 signals the position of a group of secondary osteons with a
629 different orientation. **10, 11**, general view (10) and detail (11) of the outer lateral cortex
630 showing remains of primary bone tissue. Note the irregular appearance of the external
631 surface, which exhibits ridges and valleys. **12**, transversal section showing strongly
632 remodeled tissue in the interdental bone. Note the irregular orientation of the secondary
633 osteons. 1, 2, 4, 5, 7-9, 12: cross polarized light with lambda compensator. 3, 6, 10, 11:
634 plane polarized light. Abbreviations: **ab**, alveolar bone; **ac**, acellular cementum; **cc**,
635 cellular cementum; **cl**, cementocyte lacuna; **de**, dentine; **Hb**, Haversian bone; **hl**,
636 hyaline layer; **ol**, osteocyte lacuna; **pc**, pulpar cavity; **po**, primary osteon; **ps**,

637 periodontal space; **rl**, resorption line; **Sf**, Sharpey's fibers, **vc**, vascular canal. Scale bars
638 equal 0.2 mm (1, 4, 5, 11), 0.1 mm (2, 3, 6, 8), 0.5 mm (7, 9, 10), 1 mm (12). **-PLANED**
639 **FOR A SINGLE COLUMN-**

1

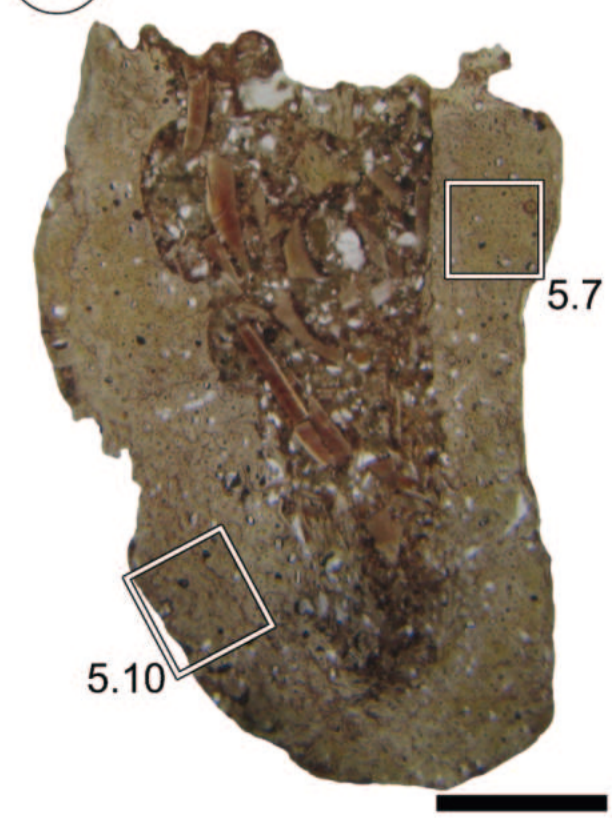
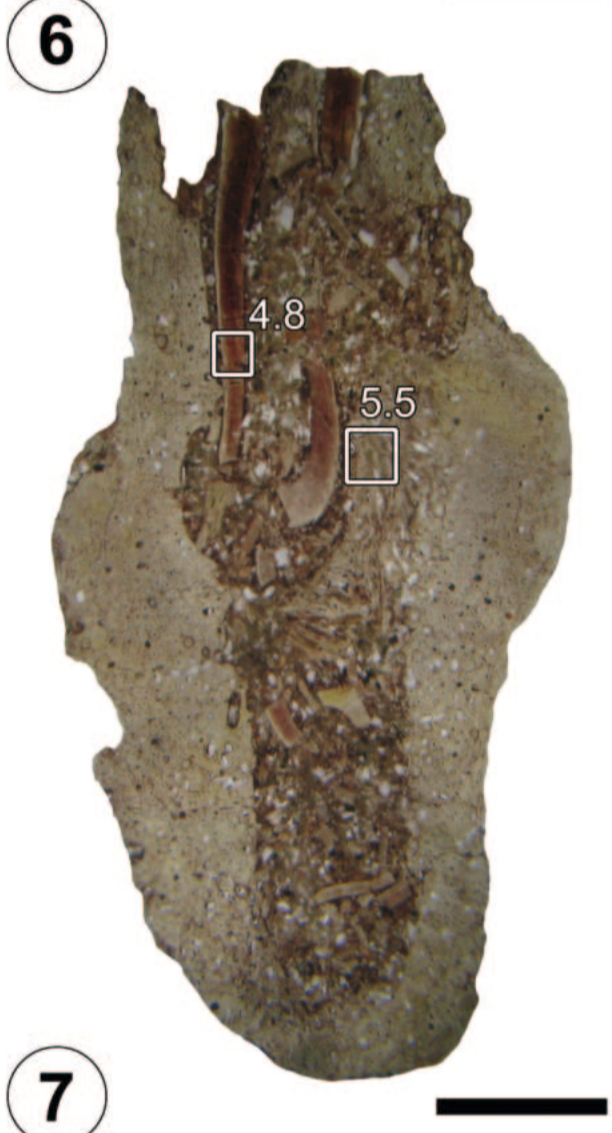
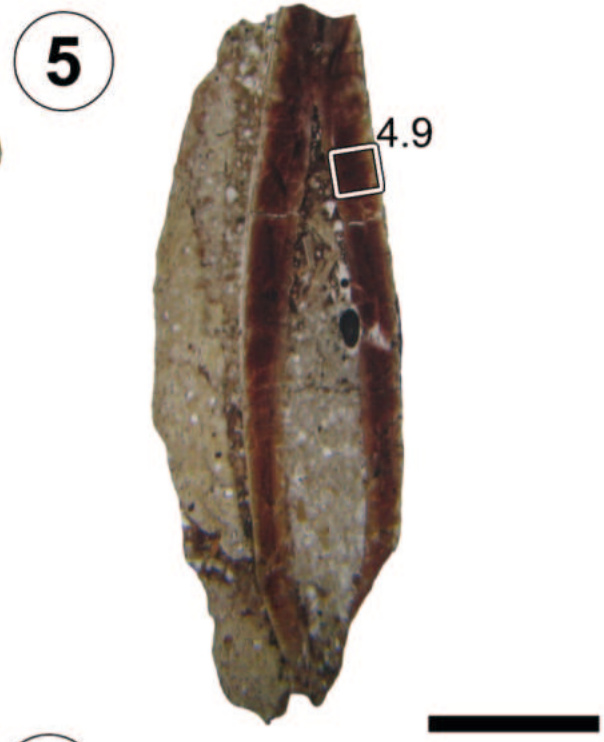
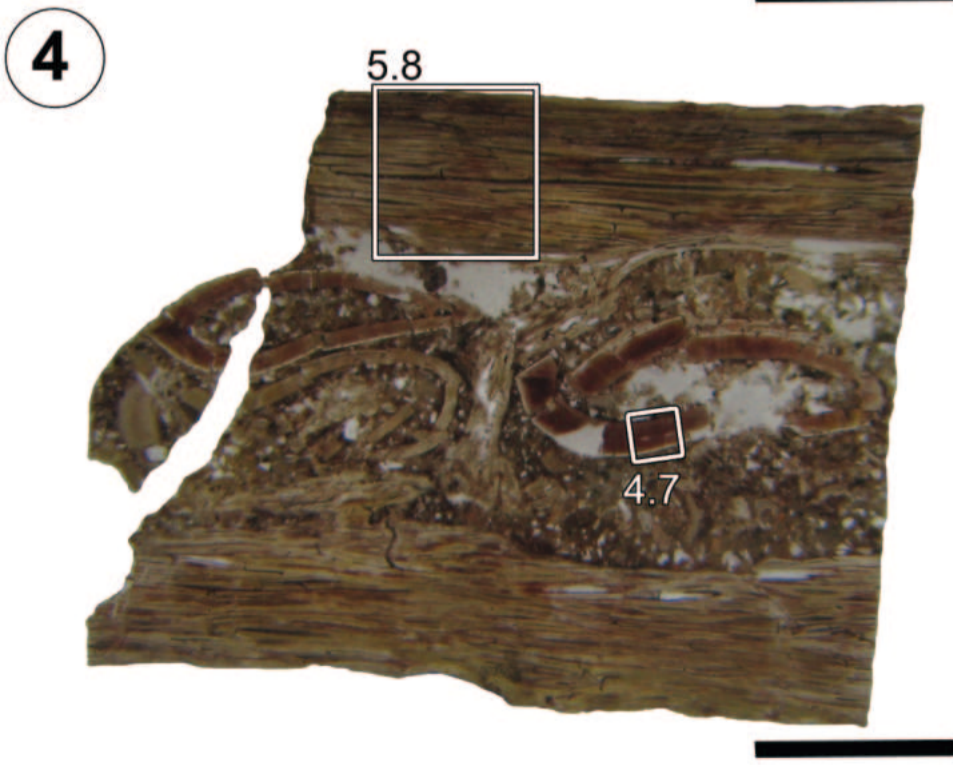
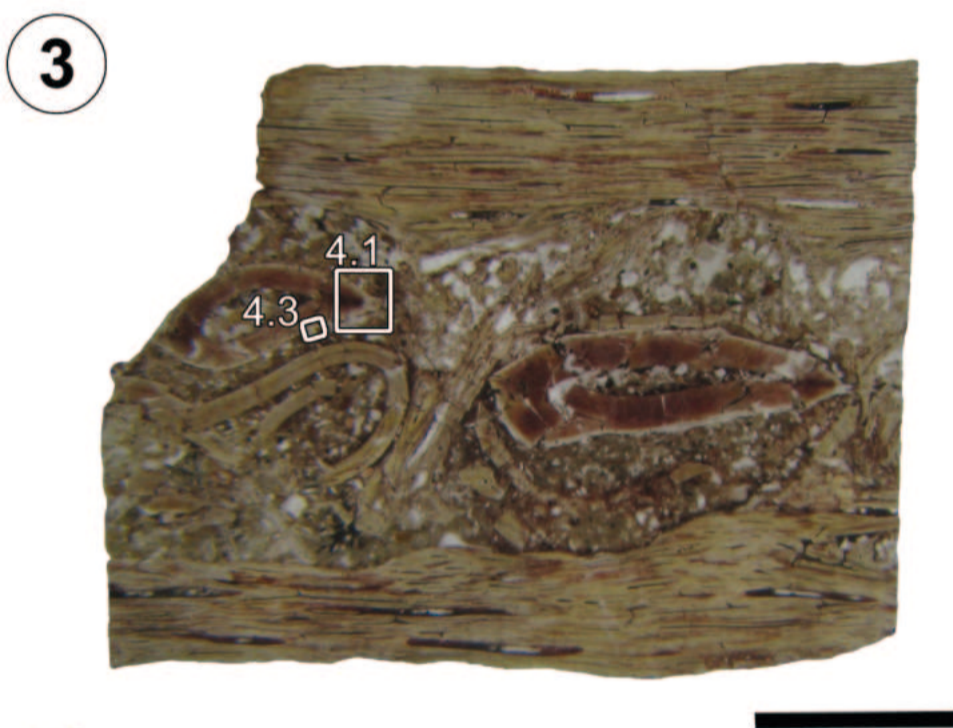
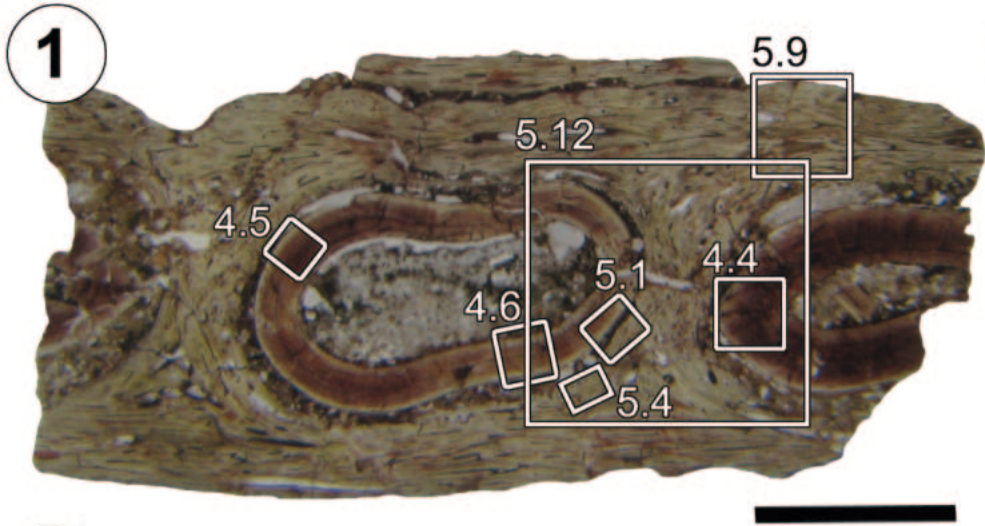


2

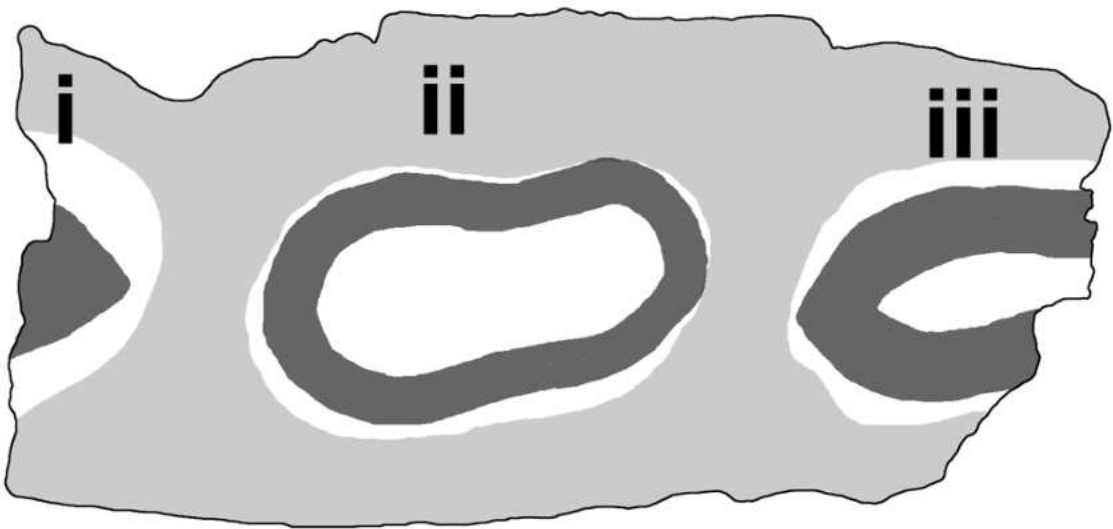


3

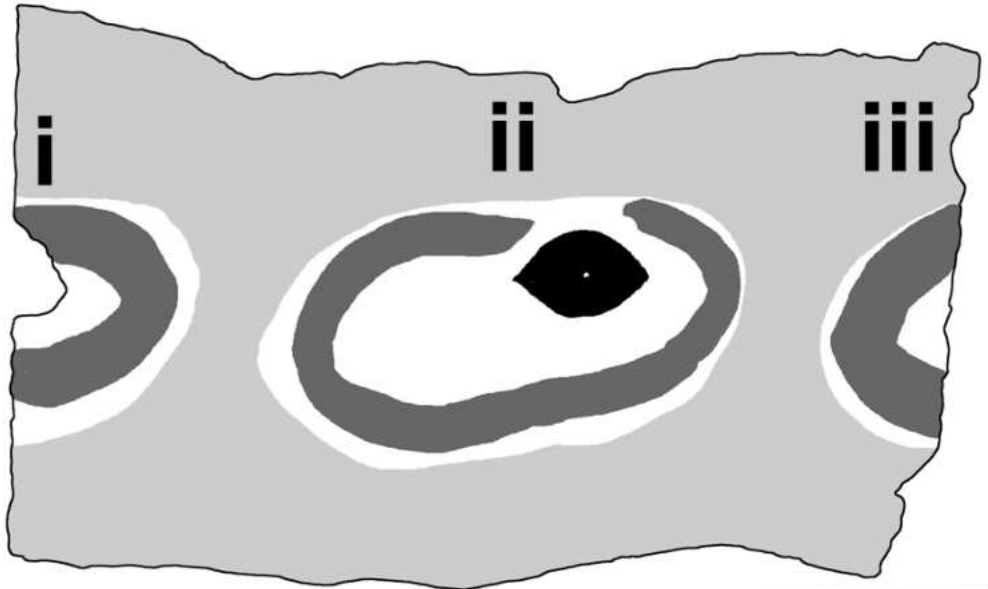




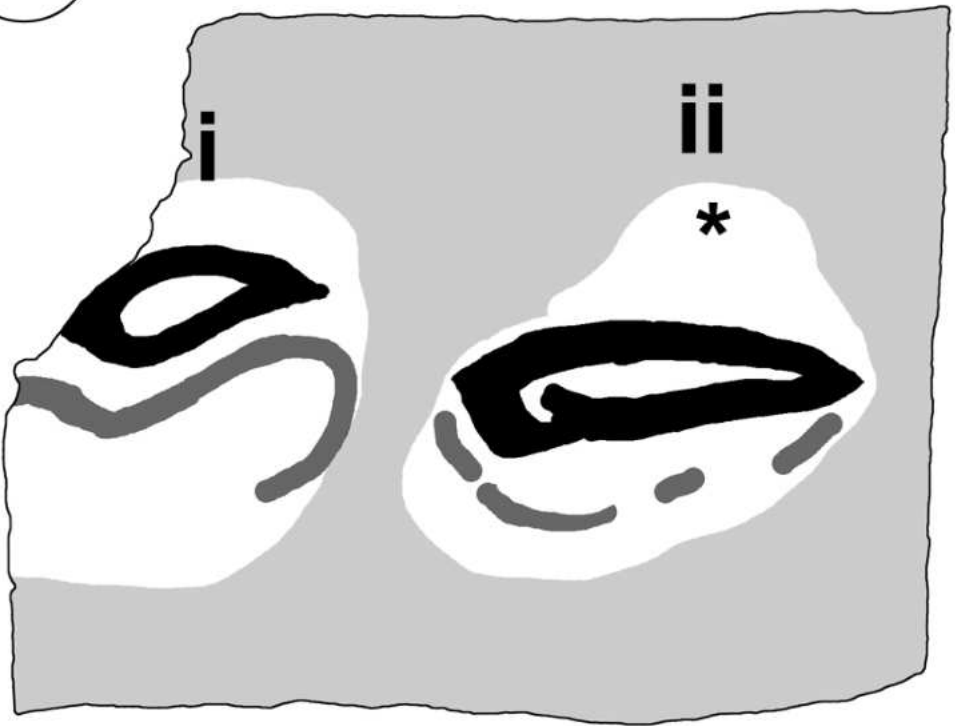
1



2



3



4

